american physiological society

JNP JOURNAL OF NEUROPHYSIOLOGY

J Neurophysiol 130: 319–331, 2023.
First published June 28, 2023; doi:10.1152/jn.00060.2023

RESEARCH ARTICLE

Control of Movement

Congruent visual cues speed dynamic motor adaptation

Sae Franklin,[1] Raz Leib,[1] Michael Dimitriou,[2] and David W. Franklin[1,3,4]

[1]*Neuromuscular Diagnostics, Department of Sport and Health Sciences, Technical University of Munich, Munich, Germany;* [2]*Physiology Section, Department of Integrative Medical Biology, Umeå University, Umeå, Sweden;* [3]*Munich Institute of Robotics and Machine Intelligence (MIRMI), Technical University of Munich, Munich, Germany; and* [4]*Munich Data Science Institute (MDSI), Technical University of Munich, Munich, Germany*

Abstract

Motor adaptation to novel dynamics occurs rapidly using sensed errors to update the current motor memory. This adaption is strongly driven by proprioceptive and visual signals that indicate errors in the motor memory. Here, we extend this previous work by investigating whether the presence of additional visual cues could increase the rate of motor adaptation, specifically when the visual motion cue is congruent with the dynamics. Six groups of participants performed reaching movements while grasping the handle of a robotic manipulandum. A visual cue (small red circle) was connected to the cursor (representing the hand position) via a thin red bar. After a baseline, a unidirectional (3 groups) or bidirectional (3 groups) velocity-dependent force field was applied during the reach. For each group, the movement of the red object relative to the cursor was either congruent with the force field dynamics, incongruent with the force field dynamics, or constant (fixed distance from the cursor). Participants adapted more to the unidirectional force fields than to the bidirectional force field groups. However, across both force fields, groups in which the visual cues matched the type of force field (congruent visual cue) exhibited higher final adaptation level at the end of learning than the control or incongruent conditions. In all groups, we observed that an additional congruent cue assisted the formation of the motor memory of the external dynamics. We then demonstrate that a state estimation-based model that integrates proprioceptive and visual information can successfully replicate the experimental data.

NEW & NOTEWORTHY We demonstrate that adaptation to novel dynamics is stronger when additional online visual cues that are congruent with the dynamics are presented during adaptation, compared with either a constant or incongruent visual cue. This effect was found regardless of whether a bidirectional or unidirectional velocity-dependent force field was presented to the participants. We propose that this effect might arise through the inclusion of this additional visual cue information within the state estimation process.

additional visual cues; force field adaptation; motor control; motor memory; state estimation

INTRODUCTION

Humans adapt to new environments and tasks by updating their motor memories to these changed conditions. Even fundamentally novel environments can be learned by the sensorimotor system through the incorporation of sensory information (1). For example, visual or proprioceptive sensory feedback can convey information regarding possible errors or rewards that trigger changes to the motor plan. Although it is clear that the motor system uses information coming from these sensory channels to understand the altered environment, especially when they carry essential or unique information, it is still unknown how additional and perhaps redundant information might also affect the adaptation of our motor memories.

It has long been clear that motor adaption to changes in task dynamics is strongly driven by proprioceptive input (2). There are many studies in which adaptation relies on proprioceptive information without the need for additional visual feedback. Critically, visually impaired people can learn new dynamics (2). Similarly, eliminating visual feedback while experiencing external forces did not affect the speed or amount of adaptation to these forces (3–5). We can also rapidly adapt our grip forces to objects' weight (6, 7) or other

Correspondence: D. W. Franklin (david.franklin@tum.de).
Submitted 6 February 2023 / Revised 19 May 2023 / Accepted 27 June 2023

generated load forces (8) without visual information regarding the object. In all of these cases, in which the sensorimotor system needs to rely on sensory inflow (reafference), motor outflow (efference or efference copy), or a combination of the two, an estimate of the current state (e.g., position and velocity) of the hand must be generated (9).

Although visual information is not essential for motor adaptation, when present it may have a significant role in the learning process. Previous studies showed the existence of motor adaptation without the need for visual information (2–4) while others showed that we can adapt our motor plans based solely on visual feedback. For example, it has been shown that participants moving in a force channel that eliminates any proprioceptive error can learn novel dynamics only with visual position error feedback (10). Similar adaptation was found in proprioceptive deafferented patients that use visual information to adapt to external forces (11–13) or visuomotor rotation (14). Moreover, these patients can use visual information to some extent to appropriately adapt their grip force and/or digit kinematics in object manipulation tasks (15, 16). It can be claimed that visual information triggers a more conscious strategy of adaptation (17), which works only in specific cases (18, 19).

Contextually relevant visual cues, such as differences in color, have been used to anticipate impending dynamics (18–22) with varying results. Although color cues appear to be effective for facilitation and switching in simple tasks such as movements in one direction (19–21), they do not allow adaptation in more complex tasks such as movements in multiple directions (18, 19). The distinction appears to arise due to the ability of color cues to be used for explicit (strategy-based) adaptation (19) that do not work in more complex tasks. In contrast, other contextually relevant visual cues such as direction of visual motion (18), lead-in movement direction (23, 24), or visual direction of movement (25) allow predictive switching between two different dynamics.

Adaptation requires accurate estimates of internal states. To produce these, it is likely that the nervous system makes favorable use of all sensory modalities at its disposal. Indeed, it is widely believed that internal representations normally rely on the statistically optimal integration of different types of sensory feedback (26, 27), although other mechanisms, such as divisive normalization (28), were suggested to explain sensory integration phenomena that cannot be explained by optimal integration. For reaching movements in particular, vision and proprioception are weighted differently based on their direction-dependent precision (29). Moreover, in the context of implicit motor adaptation, visual feedback can even lead to an appropriate modulation of muscle proprioceptive feedback itself (30, 31). In short, visual feedback can play an important role in motor adaptation.

Although visual feedback is not essential for motor learning, there is some evidence that it can affect the learning rate. Vision, combined with proprioceptive information, can improve the estimation regarding changes in the environment. The upgraded estimation can allow for faster learning as we can predict the perturbation in following movements. For example, in tasks involving visual shift of the hand spatial position, participants learn the perturbation slower when the visual information regarding hand position was blurry compared with sharp (32, 33). This example demonstrates that visual information affects the uncertainty that we have regarding the observed information and change our ability to modify the internal representation of the environment.

Here, we further investigate the role of visual cues on the sensorimotor control system during adaptation to consistent (nonswitching) dynamics. In contrast with previous studies that tested the effect of arbitrary (34) or distorted visual cues (5), we contrasted the effect of providing congruent (potentially meaningful) versus incongruent visual cues. We assessed how the existence of additional visual cues could affect the speed of adaptation to different force field types of varying complexity (unidirectional and bidirectional). Importantly, we tested two different force fields and two visual cues such that we can determine whether it is the specific type of visual cue or the congruent nature of the cue that drives any specific difference in adaptation. Specifically, we tested if a visual cue that is congruent or incongruent with the experienced forces affects the learning of novel force field dynamics. We hypothesized that congruent visual cues would speed adaptation regardless of the complexity of the force field as it provides an additional visual cue consistent with the proprioceptive information and underlying force field dynamics.

MATERIALS AND METHODS

Participants

Sixty neurologically healthy, right-handed (35) human participants (34 males and 26 females) took part in the experiment (mean age of 24.3 ± 5.5 yr). All participants were naïve as to the purpose of the study and gave their written informed consent before participating. Each participant participated in one experimental session of ~45 min each and was randomly assigned to one of the six conditions. The institutional ethics committee at the University of Cambridge approved the study.

Experimental Apparatus and Setup

Participants were firmly strapped into an adjustable chair in front of a robotic rig (Fig. 1*A*). They made reaching movements with their right arm in the horizontal plane at ~10 cm below their shoulder level while the forearm was supported against gravity with an air sled. Participants grasped the handle of a vBOT robotic interface, which was used to generate the environmental dynamics. The vBOT manipulandum is a custom-built planar robotic interface that can measure the position of the handle and generates forces on the hand (36). A six-axis force transducer (ATI Nano 25; ATI Industrial Automation) measures the endpoint forces applied by the participant at the handle. The position of the vBOT handle was calculated from joint-position sensors (58SA; IED) on the motor axes. Position and force data were sampled at 1 kHz. Visual feedback was provided using a computer monitor mounted above the vBOT and projected into the plane of the movement via a mirror. This virtual reality system covers the manipulandum, arm, and hand of the participant, which obscures the location of the arm from their view.

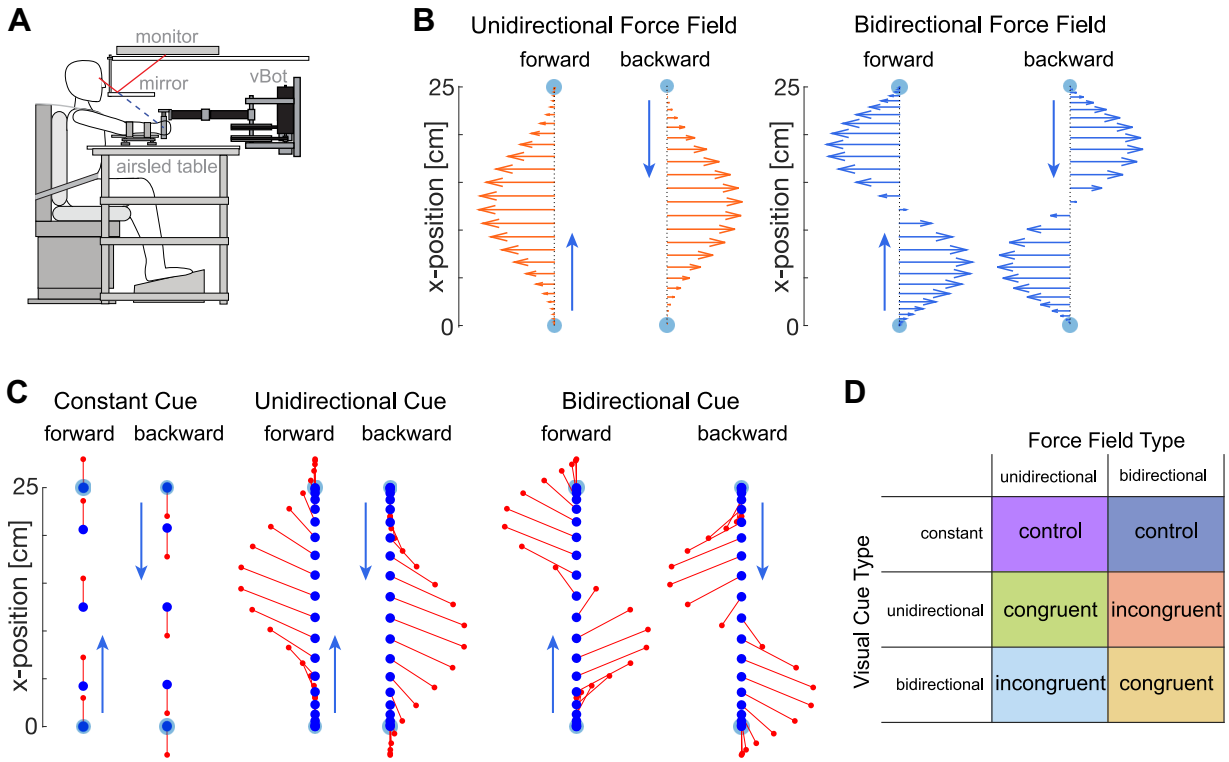

Figure 1. Experimental setup. *A*: participants were seated and grasped the handle of a robotic manipulandum with their right hand. Visual feedback about the task and the location of their hand was provided through a monitor reflected by a mirror such that it appeared in the plane of movement. The arm was supported by an airsled on a table. *B*: two types of force fields were applied during an exposure phase. Three groups of participants performed movements within a unidirectional velocity-dependent force field (*left*). Three other groups of participants performed movements in a bidirectional velocity-dependent force field in which the sign of the forces switched halfway through the movement (*right*). *C*: visual cues presented during movements depending on the group. Each of three groups for each force field was provided with a different visual cue during the movements. This visual cue was either constant (*left*), unidirectional (*middle*), or bidirectional (*right*). The diagram shows the visual feedback presented at different points (times) in the movement if participants made a straight movement between the targets during the exposure phase. In the preexposure and postexposure phases, all groups were presented with the constant cue. *D*: six groups of participants performed the experiments with all possible combinations of visual cue type and force field type resulting in a control group, congruent group, and incongruent group for each force field type.

Experimental Paradigm

Participants made alternating forward and backward point-to-point reaching movements between two targets. The participant initiated each trial by moving the cursor (yellow circle of 0.5 cm radius representing the participant's hand position) into the start circle (gray circle of 0.7 cm radius which became white once participants had moved the cursor into the start circle). A small red circle (radius 0.3 cm) was visually attached to the end of the cursor via a thin red bar. This visual cue was located 2 cm directly in front of the cursor (in the direction of movement) when participants were at rest but varied depending on the experimental condition. The start circle, target circle, and cursor were shown from the beginning of each trial. Once participants had maintained the cursor within the start circle for 1 s, a tone signaled to the participant to initiate a movement to a white target circle (radius 0.8 cm) located 25.0 cm away. On each trial, participants were required to reach the target within an allocated time window to subsequently maintain the cursor within the target for 400 ms before the trial was determined to be finished. Visual feedback was then provided about the success of the previous trial. A trial was considered successful if participants did not overshoot the target, and the duration of the movement (between exiting the start and entering the target) was between 625 and 775 ms. On successful trials, the participants received positive feedback. Specifically, if the movement duration was between 662.5 and 737.5 ms, "great" was presented visually on the monitor, otherwise "good" was presented. In both cases, a point counter increased by one. In the case of an unsuccessful trial, other messages were provided visually at the end of each trial to inform the participants of their performance (either "too fast," "too slow," or "overshot target"). All visual messages were presented for 500 ms, except for the point counter which was continuously presented. All trials were analyzed regardless of their success. Undershooting the target was not specifically penalized as this generally would extend the duration of the movement (which requires entering the target) and therefore the duration would no longer be successful.

Participants were provided with rest breaks every 200 trials. In the absence of any specific intervention by the participants, trials immediately followed after the previous trial (minimum 1.9 s time between movements: 400 ms hold phase in the target + 500 ms intertrial interval + 1.0 s waiting in the start circle). However, participants were also able to take additional rest breaks at any point in time by moving the cursor out of the starting circle.

Protocol

Participants were randomly assigned to one of six groups ($n = 10$). Participants performed alternating forward and backward reaching movements in three phases of the experiment: preexposure (10 blocks), exposure (30 blocks), and postexposure (5 blocks). Blocks consisted of 12 movements (6 forward and 6 backward reaches) such that each participant performed 540 movements in total. These 12 movements consisted of 10 movements in the environmental dynamics (null field or force field) and 2 movements in a mechanical channel (1 in each direction of movement), which were positioned randomly within the 12 trials. The mechanical channel (37, 38) was implemented as a mechanical channel resisting lateral motion with a spring constant of 5,000 N/m and a damping coefficient of 2 Ns/m. Both the preexposure and postexposure phases were performed in the null field.

All groups experienced a velocity-dependent force field during the exposure phase. This force field was a curl force field scaled by a value k, which varied throughout the movement as a function of the distance d between the start and target position:

$$\begin{bmatrix} F_x \\ F_y \end{bmatrix} = k \begin{bmatrix} 0 & 1 \\ -1 & 0 \end{bmatrix} \begin{bmatrix} \dot{x} \\ \dot{y} \end{bmatrix} \quad (1)$$

Three of the groups experienced a unidirectional velocity-dependent force field during the exposure phase (Fig. 1*B*, *left*). In the unidirectional force field, the value k varied as:

$$k = \left(\frac{2.7d^2}{l^2}\right) - \left(\frac{5.4d^3}{l^3}\right) + \left(\frac{2.7d^4}{l^4}\right) \quad (2)$$

where $0 \leq d \leq l$ and the length of movement $l = 25$.

The other three groups were presented with a bidirectional velocity-dependent force field during the exposure phase (Fig. 1*B*, *right*) where k was defined as:

$$k = \left(\frac{5.4d}{l^2}\right) - \left(\frac{16.2d^2}{l^3}\right) + \left(\frac{10.2d^3}{l^4}\right) \quad (3)$$

The direction of the force field was varied for half of the participants in each group by changing the sign of k. These two force fields were selected to match the two types of visual cues that were presented, such that the cues could either match the force field (congruent) or not match the force field (incongruent).

Each group was presented with a visual cue throughout the experiment (Fig. 1*C*). The visual cue was a red circle that was connected by a thin red line to the cursor. For one of the unidirectional field groups and one of the bidirectional field groups, the location of the red circle was located $x = 0, y = \pm 2$ cm relative to the cursor (constant cue). That is, for forward movements, it was located at $y = +2$ cm, whereas for backward movements it was located at $y = -2$ cm. For the other four groups (two unidirectional and two bidirectional), the visual cue was located $x = k, y = \pm 2$ cm relative to the cursor, where k was defined using either *Eq. 2* or *Eq. 3*. Specifically, for the two unidirectional force field groups, this visual cue could either be also unidirectional (congruent cue) or bidirectional (incongruent cue). Similarly, for the bidirectional force field, the cue was either unidirectional (incongruent) or bidirectional (congruent). The six different conditions (force field and visual cue) can be seen in a video (Supplemental Video S1 https://doi.org/10.6084/m9.figshare.22843799). For all groups, the value k was set to zero during the preexposure and postexposure trials. This meant that during null field movements, the visual cue was always located 2 cm away from the cursor for all six groups. Overall, six groups of participants combined all possible combinations of visual cue type and force field type resulting in a control group, congruent group, and incongruent group for each force field type (Fig. 1*D*).

Analysis

The data were analyzed using Matlab R2019a. Force and kinematic data were low-band pass filtered with a fifth-order, zero phase-lag Butterworth filter with a 40-Hz cutoff. Individual trials were aligned on movement onset. For each trial, we calculated measures of kinematic error or force compensation between 200 ms before leaving the start position until 200 ms after entering the target position.

For each nonchannel trial, the absolute maximum perpendicular error (MPE) was calculated and used as a measure of the kinematic error. The MPE is the absolute maximum perpendicular distance between the hand trajectory and the straight line between the start and end targets. As this measure only assesses a single point in the trajectory, we also calculate the absolute hand path error (39) that reflects the sum of the absolute distance away from the straight-line trajectory throughout the entire movement. Specifically, this was calculated between the start and target positions as:

$$\int_{t=t_0}^{t_f} |x(t)||\dot{y}(t)|dt$$

The absolute hand path error was calculated from the start of the movement, t_0 (200 ms before exiting the start circle) to the end of the movement, t_f (200 ms after entering the target circle).

To assess feedforward learning independent of co-contraction, we analyzed the force compensation to the force field produced on channel trials (40). Force compensation is calculated by the regression between the force produced by participants into the wall of the simulated channel (lateral measured force) and the force needed to compensate exactly for the force field. Here, the perfect compensatory endpoint force is determined on each trial using the forward velocity on each trial, and the magnitude of the force field k as calculated by *Eqs. 2* and *3*. Here, values in the null force field before learning (preexposure phase) should be close to zero.

We performed hypothesis-based planned comparisons and consider significance at the $P < 0.05$ level for all statistical tests. ANOVAs were examined in JASP 0.17.1. For both the maximum perpendicular error, absolute hand path error, and the force compensation values, we performed an ANOVA with the main factors of force field (2 levels: unidirectional and bidirectional) and condition (3 levels: constant, congruent, and incongruent) on the final levels at the end of adaptation (final 10 blocks). Where applicable we perform post hoc comparisons (Tukey).

To examine differences in the time constant of adaptation and final asymptote, we fit an exponential function to the force compensation for each trial throughout the adaptation phase of the experiment. To generate confidence intervals

for our parameter estimates, we performed block bootstrapping in which we left out each possible set of two participants from each group and fitted the remaining eight. We used the distribution of parameters across these 45 fits to estimate the confidence limits. To test whether each parameter varied between the two groups, we generated all possible differences in each parameter from our bootstrap to generate a new bootstrap sample (45 × 45 samples). This commonly used technique (19, 41) is used as a single participant's data are often too noisy to obtain an accurate estimate of the learning parameters. Differences in the magnitude and speed of learning were contrasted only across the same force fields.

Model

To interpret these results, we suggest a framework in which the force field adaptation is based on estimating the scaling factor k using a state estimator. The state estimator integrates proprioceptive and the visual representation of the forces to estimate the nature of the dependency of the scaling factor on the hand position while reducing the effect of any sensory noise. To simplify the problem, we suggest that the state estimator needs to estimate the coefficients of the polynomials describing the scaling factor. That is, for the unidirectional velocity-dependent force field, the state estimator needs to estimate the values $C_{uni} = [2.7, -5.4, 2.7]^T$, and for the bidirectional velocity-dependent force field, the values $C_{bi} = [5.4, -16.2, 10.2]^T$. The observation, which is the input to the state estimator, includes proprioceptive and visual information about the scaling factor depending on the experimental condition. For the constant visual information conditions, which served as the control conditions, we did not provide the model with additional visual information about the force magnitude. In these conditions, the visual information given to the participants was a shifted version of their hand position and thus did not convey any information regarding the force magnitude. The mathematical formulation of the observation across all conditions was represented as:

$$y^{(n)} = x^{(n)T}c + \varepsilon^{(n)} \tag{4}$$

where $y^{(n)}$ is the observations on the n-th trial, $x^{(n)}$ is a vector representing the position dependency of the scaling factor, that is, $x_{uni}^{(n)} = \left[\frac{d^{(n)2}}{l^2} \quad \frac{d^{(n)3}}{l^3} \quad \frac{d^{(n)4}}{l^4}\right]$ for the unidirectional case and $x_{bi}^{(n)} = \left[\frac{d^{(n)}}{l^2} \quad \frac{d^{(n)2}}{l^3} \quad \frac{d^{(n)3}}{l^4}\right]$ for the bidirectional case. $\varepsilon^{(n)}$ represents random additive noise with normal distribution, $\varepsilon^{(n)} \sim N(0, R)$ where R represents the variance-covariance noise matrix. The R matrix was set as a diagonal matrix with values of 0.1 on the diagonal. Thus, we assume the same level of noise for both proprioceptive and visual sensory modalities.

We implemented the state estimator as a Kalman filter (42). We initiate the system with an initial coefficients estimation, in this case, since the force field was turned on without any prior notice, we set the values to zero, $\hat{c}^{(1|0)} = [0, 0, 0]$ and noise added to proprioceptive or visual information as Gaussian noise with zero mean and 0.1 variance. Between experimental conditions, we varied the initial uncertainty regarding the estimation. That is $p^{(1|0)}$ was a diagonal matrix with different values between conditions. For the control condition and congruent condition, we set the uncertainty values to 5 and 10, respectively, for both the unidirectional and bidirectional force field. This means that for the congruent condition, since both the visual and proprioceptive modalities are providing the same information, the initial estimation of a null force field is more uncertain than for the control condition in which the information is providing only via a single information modality. In this case of higher uncertainty, the initial estimation is rapidly replaced with a more certain estimation. For the incongruent conditions, we set the initial uncertainty to 1.5 and 1 for the unidirectional and bidirectional force fields, respectively. In the case of incongruent visual information, we assume that the visual information is reducing the uncertainty regarding the initial estimation since the visual and proprioceptive information are not aligned, which requires gathering more information so to update the estimation. In this case, the rate of adaptation will be slower than the learning rate in the congruent condition, or both the congruent and control conditions. To update the estimation, we used the Kalman algorithm.

$$\begin{aligned} k_f^{(n)} &= p^{(n|n-1)}x^{(n)} \cdot \left(x^{(n)T}p^{(n|n-1)}x^{(n)} + R\right)^{-1} \\ \hat{c}^{(n|n)} &= \hat{w}^{(n|n-1)} + k_f^{(n)}\left(y^{(n)} - x^{(n)T}\hat{c}^{(n|n-1)}\right) \\ p^{(n|n)} &= \left(I - k_f^{(n)}x^{(n)T}\right)p^{(n|n-1)} \end{aligned} \tag{5}$$

For each trial, the observation included four different points along the trajectory which were chosen randomly. Based on these four points, we updated the coefficients estimation using the Kalman filter gains k_f. Changing the number of points which are used in each trial affects the number of trials needed for the estimations to converge but not the nature of the estimation process. That is, reducing the number of points used in each trial will increase the number of trials needed and vice versa. Based on the estimated coefficients, we estimated the scaling factor, $\hat{k} = x^T\hat{c}$, for each trial using 250 equally spaced points along the movement path and calculated the mean square error between it and the scaling factor that was used in each experimental condition.

$$MSE(n) = \frac{1}{250}\sum_{i=1}^{250}\left(k - \hat{k}^{(n)}\right)^2 = \frac{1}{250}\sum_{i=1}^{250}\left(k - x^{(i)T}\hat{c}^{(n)}\right)^2 \tag{6}$$

We run 10 simulations for each condition same as the number of participants in each experimental group.

RESULTS

Six groups of participants performed alternating forward and backward discrete movements of the arm between two targets, with a small red circle (visual cue) connected to the cursor. After initial movements in a null field, either a unidirectional (3 groups) or bidirectional (3 groups) velocity-dependent force field was applied during the movements. In each force field, the three groups were presented with the visual cue representing the force field (congruent cue), representing a different force field (incongruent cue), or unaffected (constant cue). Finally, the force field was removed (null field) and the visual cue was constant in all groups.

Measures of Adaptation

In the preexposure phase, all six groups of participants performed relatively straight movements to the targets with little lateral kinematic error (Fig. 2, *A* and *C*). As the participants were exposed to the force fields (exposure phase), the kinematic errors increased initially but reduced with further experience in the force fields. The initial MPE upon exposure to the force field (first 10 trials) was not significantly different across field type ($F_{1,54} = 0.179$; $P = 0.674$; $\eta^2 = 0.003$), condition ($F_{2,54} = 2.127$; $P = 0.129$; $\eta^2 = 0.072$), or interaction between force field and condition ($F_{2,54} = 0.222$; $P = 0.802$; $\eta^2 = 0.008$). Several major effects are visible in the data. First, there are clear differences in the reduction of kinematic error between the two force fields (unidirectional reduces error further than bidirectional). Second, for both force fields, it appears that the congruent groups (yellow and green) learn slightly better (stronger reduction in MPE) than either the control (dark blue or purple) or incongruent (red and light blue) groups. The final level of MPE (last 10 blocks, Fig. 2, *B* and *D*) was examined with an ANOVA with main factors of force field (2 levels) and condition (3 levels). There was a main effect of force field ($F_{1,54} = 61.574$; $P < 0.001$; $\eta^2 = 0.5$), but the main effect of condition failed to reach significance ($F_{2,54} = 2.999$; $P = 0.058$; $\eta^2 = 0.049$), and there was no interaction effect ($F_{2,54} = 0.831$; $P = 0.441$; $\eta^2 = 0.013$). Therefore, there is a strong effect of the force field on the reduction of the kinematic error during adaptation, but no clear evidence for differences across the three conditions. Finally, we examined whether the aftereffects (first 10 trials upon removal of the force field) were different across the conditions. As expected, there was an effect of force field ($F_{1,54} = 62.017$; $P < 0.001$; $\eta^2 = 0.522$), but we found no effect of condition ($F_{2,54} = 0.608$; $P = 0.548$; $\eta^2 = 0.010$) or of an interaction effect ($F_{2,54} = 0.765$; $P = 0.470$; $\eta^2 = 0.013$). Overall, the presence of a congruent visual cue affected the final adaptation but had no effect on the aftereffects.

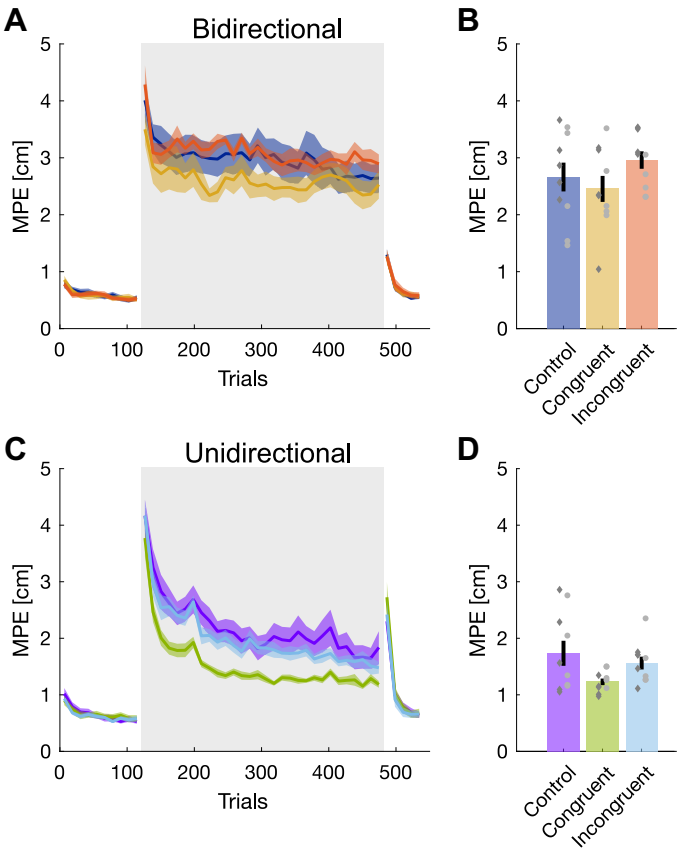

Figure 2. Kinematic error during adaptation. *A*: absolute maximum perpendicular kinematic error throughout the experiment in the bidirectional force fields for the control (dark blue), congruent (yellow), and incongruent (red) groups. The mean (solid line) and standard deviation of the mean (shaded regions) across participants for each block in the experiments is shown. Shaded gray region indicates the period of force field exposure. *B*: final levels of absolute maximum perpendicular error (MPE) at the end of the exposure phase (last 10 blocks). Error bars are standard error of the mean, and individual points represent individual participants with the color indicating the direction of the force field (light gray circles: positive *k*; dark gray diamonds: negative *k*). *C*: absolute maximum perpendicular kinematic error in the unidirectional force fields for the control (purple), congruent (green), and incongruent (light blue) groups. *D*: final levels of absolute maximum perpendicular error at the end of the exposure phase (last 10 blocks).

Similar results were found for the absolute hand path error, which considers errors throughout the whole trajectory (Fig. 3). Although the initial error upon exposure to the force field showed a small but significant difference according to the force field ($F_{1,54} = 5.372$; $P = 0.024$; $\eta^2 = 0.085$), there was no effect of condition ($F_{2,54} = 1.178$; $P = 0.316$; $\eta^2 = 0.037$) or interaction ($F_{2,54} = 0.735$; $P = 0.484$; $\eta^2 = 0.023$). The final level of absolute hand path error (last 10 blocks, Fig. 3, *B* and *D*) was examined with an ANOVA with main factors of force field (2 levels) and condition (3 levels). Similar to MPE, there was a main effect of force field ($F_{1,54} = 54.879$; $P < 0.001$; $\eta^2 = 0.477$), but the main effect of condition failed to reach significance ($F_{2,54} = 1.902$; $P = 0.159$; $\eta^2 = 0.033$), and there was no interaction effect ($F_{2,54} = 1.130$; $P = 0.331$; $\eta^2 = 0.020$). However, we found significant differences during the aftereffects for both force field ($F_{1,54} = 14.741$; $P < 0.001$; $\eta^2 = 0.178$) and condition ($F_{2,54} = 4.364$; $P = 0.018$; $\eta^2 = 0.106$) but not for their interaction ($F_{2,54} = 2.60$; $P = 0.084$; $\eta^2 = 0.063$). Post hoc comparisons (Tukey) found that the aftereffects were smallest in the control condition (both $P < 0.047$), but no differences between the congruent and incongruent conditions ($P = 0.971$).

To investigate the predictive compensation to the force fields independent of factors such as limb inertia or increases in co-contraction, we examined the force compensation throughout the experiment (Fig. 4). During the initial preexposure phase, the force compensation (relative to adapting to the subsequent force fields) remained close to zero as expected. Upon the start of the exposure phase, the force compensation for all groups increases, with a larger increase in the unidirectional force field groups (around 60%, Fig. 4*C*) compared with the bidirectional force field groups (around 30%, Fig. 4*A*). However, again both congruent visual cue groups have higher levels of force compensation at the end of adaptation compared with other groups with the same force field. The final level of force compensation (last 10 blocks, Fig. 4, *B* and *D*) was examined with an ANOVA with main factors of force field (2 levels) and condition (3 levels). There were main effects of both force field ($F_{1,54} = 191.968$; $P < 0.001$; $\eta^2 = 0.741$) and condition ($F_{2,54} = 5.491$; $P = 0.007$; $\eta^2 = 0.042$), with no interaction effect ($F_{2,54} = 1.107$; $P = 0.338$; $\eta^2 = 0.009$). Therefore, there is a strong effect of the force field on the reduction of the kinematic error during adaptation, but also

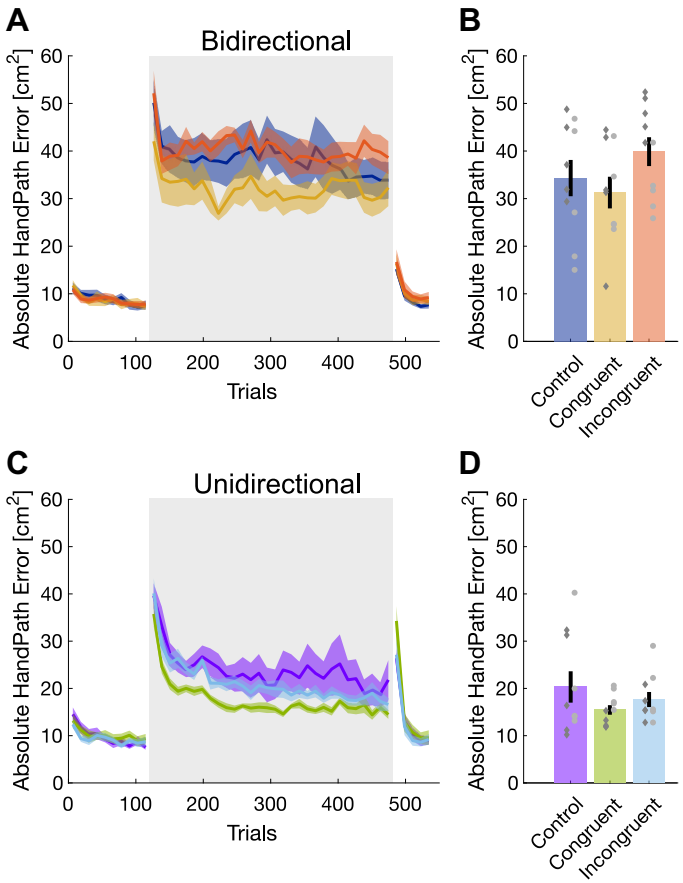

Figure 3. Absolute hand path error during adaptation. *A*: sum of the absolute hand path error throughout the experiment in the bidirectional force fields for the control (dark blue), congruent (yellow), and incongruent (red) groups. The mean (solid line) and standard deviation of the mean (shaded regions) across participants for each block in the experiments is shown. Shaded gray region indicates the period of force field exposure. *B*: final levels of absolute hand path error at the end of the exposure phase (last 10 blocks). Error bars are standard error of the mean, and individual points represent individual participants with the color indicating the direction of the force field (light gray circles: positive *k*; dark gray diamonds: negative *k*). *C*: absolute hand path error in the unidirectional force fields for the control (purple), congruent (green), and incongruent (light blue) groups. *D*: final levels of absolute hand path error at the end of the exposure phase (last 10 blocks).

clear evidence for differences across the three conditions. A post hoc comparison (Tukey) demonstrated that the congruent conditions had significantly higher force compensation than either the control ($P = 0.03$) or incongruent conditions ($P = 0.009$) but that there were no differences between the control and incongruent conditions ($P = 0.896$) across the different force fields. However, despite the differences in the final level of adaptation, there was only a main effect of force field ($F_{1,54} = 20.452$; $P < 0.001$; $\eta^2 = 0.274$) on the magnitude of aftereffects, with no effect of condition ($F_{2,54} = 0.099$; $P = 0.906$; $\eta^2 = 0.003$) or interaction ($F_{2,54} = 0.056$; $P = 0.946$; $\eta^2 = 0.001$). Overall, despite adapting to the same force fields and having the same visual presentation of the cursor representing hand position, participants that we also presented with an additional visual cue that matched the force field adapted more to the force fields (independent of the type of force field). That is, although all groups received visual feedback of the cursor motion (providing visual information regarding the errors induced by the force fields), additional congruent visual motion assists with the formation of the motor memory of the external dynamics. However, such differences were not found in the size of aftereffects.

Learning Rates

The force compensation in the exposure phase was fit with an exponential function to determine the time contrast of adaptation and final asymptote levels for the six groups (Fig. 5). For the bidirectional force field (Fig. 5, *A–C*), we find a higher final asymptote for the congruent compared with the control ($P = 0.044$) and incongruent ($P < 0.001$) groups, but also for the control compared with the incongruent group ($P = 0.0108$). However, we find no differences in the time constant of adaptation across all three groups (all $P > 0.16$). For the unidirectional force field (Fig. 5, *D–F*), we also find strong differences in the asymptote, with a larger

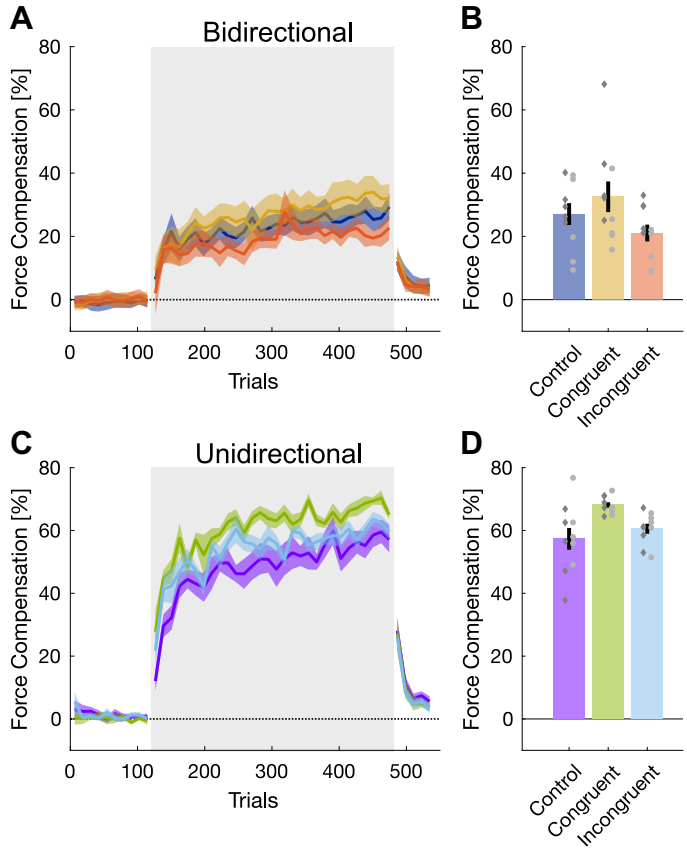

Figure 4. Predictive force compensation during adaptation. *A*: force compensation as measured on channel trials throughout the experiment in the bidirectional force fields for the control (dark blue), congruent (yellow), and incongruent (red) groups. The mean (solid line) and standard deviation of the mean (shaded regions) across participants for each block in the experiments is shown. Shaded gray region indicates the period of force field exposure. *B*: final levels of force compensation at the end of the exposure phase (last 10 blocks). Error bars are standard error of the mean, and individual points represent individual participants with the color indicating the direction of the force field (light gray circles: positive *k*; dark gray diamonds: negative *k*). *C*: force compensation in the unidirectional force fields for the control (purple), congruent (green), and incongruent (light blue) groups. *D*: final levels of force compensation at the end of the exposure phase (last 10 blocks).

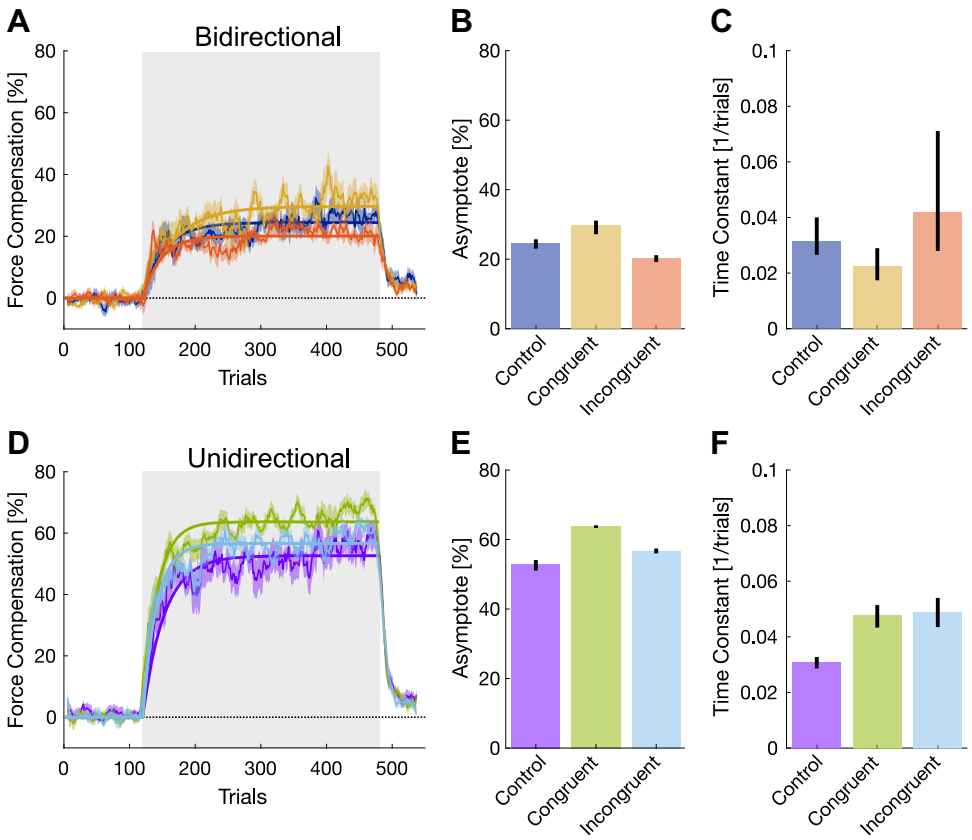

Figure 5. Exponential fit of adaptation. *A*: bidirectional force field groups. The best-fit exponential curve during the exposure phase of the experiment (solid line) and the mean and standard error of the mean across trials (thin line and shaded region) is shown. Shaded gray region indicates the period of force field exposure. *B*: the mean best-fit asymptote for each of the three bidirectional force field groups. Error bars represent 95% confidence intervals of the parameters. *C*: the mean best-fit time constant for each of the three bidirectional force field groups. Error bars represent 95% confidence intervals of the parameters. *D*: the best-fit exponential curve during adaptation to the unidirectional force field groups. *E*: the best-fit asymptote for each of the three unidirectional force field groups. *F*: the best-fit time constant for each of the three unidirectional force field groups.

adaptation for the congruent compared with the control ($P < 0.001$) or incongruent groups ($P < 0.001$), but here the incongruent group showed higher adaptation than the control group ($P < 0.001$). The rates of adaptation to the unidirectional force field were higher for the congruent and incongruent groups than the control group (both $P < 0.001$) but with no difference between them ($P = 0.436$).

Model Results

We simulated the learning process for each of the experimental conditions using state estimation-based learning. In this learning scheme (Fig. 6*A*), the state estimator integrates information from multiple sensory modalities, if available, to estimate the scaling factor from noisy observations. Examples of datasets available to the state estimator according to each experimental condition are depicted in Fig. 6*B*. Using these datasets, the state estimator estimates the scaling factor that determines the level of adaptation to the force field. We calculated the difference between estimated and actual scaling factors. Figure 6*C* shows the learning trends for each condition during adaptation to the unidirectional force field. For this adaptation protocol, the trends predicted by the model are similar to the experimental observed trends (Figs. 2 and 4). We found that for the congruent condition, the scaling factor estimation converges faster than the other conditions, as in this condition, the state estimation can use both proprioceptive and visual information together with higher sensitivity to the observation. For the incongruent condition, we found that lower observation sensitivity can lower the learning rate. This lower sensitivity is due to our assumption regarding the reliability of the observations during this condition which are opposite to each other. For adaption to the bidirectional force field, we found again a faster adaptation rate for the congruent condition compared with the incongruent and control conditions (Fig. 6*D*). Here, we simulated even lower observation sensitivity for the incongruent condition which resulted in a learning rate which was slower compared with the control condition.

We also found that the ability of the state estimation to accurately estimate the scaling factor of the bidirectional force field was reduced compared with the unidirectional force field. This slower adaptation for the bidirectional force field was also evident in the experimental results (Figs. 2 and 4). This difference between force fields was evident even for conditions in which parameters had the same values, for example, in the congruent and control conditions.

DISCUSSION

In this study, we examined whether additional visual information regarding the nature of external dynamics affects the rate of adaptation to these forces. We provided participants with online visual representation of forces that could accurately or falsely represent the experienced forces and examined if these visual cues assist force field adaptation, especially when the cues were congruent with the experienced forces. Three groups experienced a unidirectional force field, whereas the other three groups experienced a bidirectional force field. Using these unidirectional or bidirectional velocity-dependent force fields, we have compared different

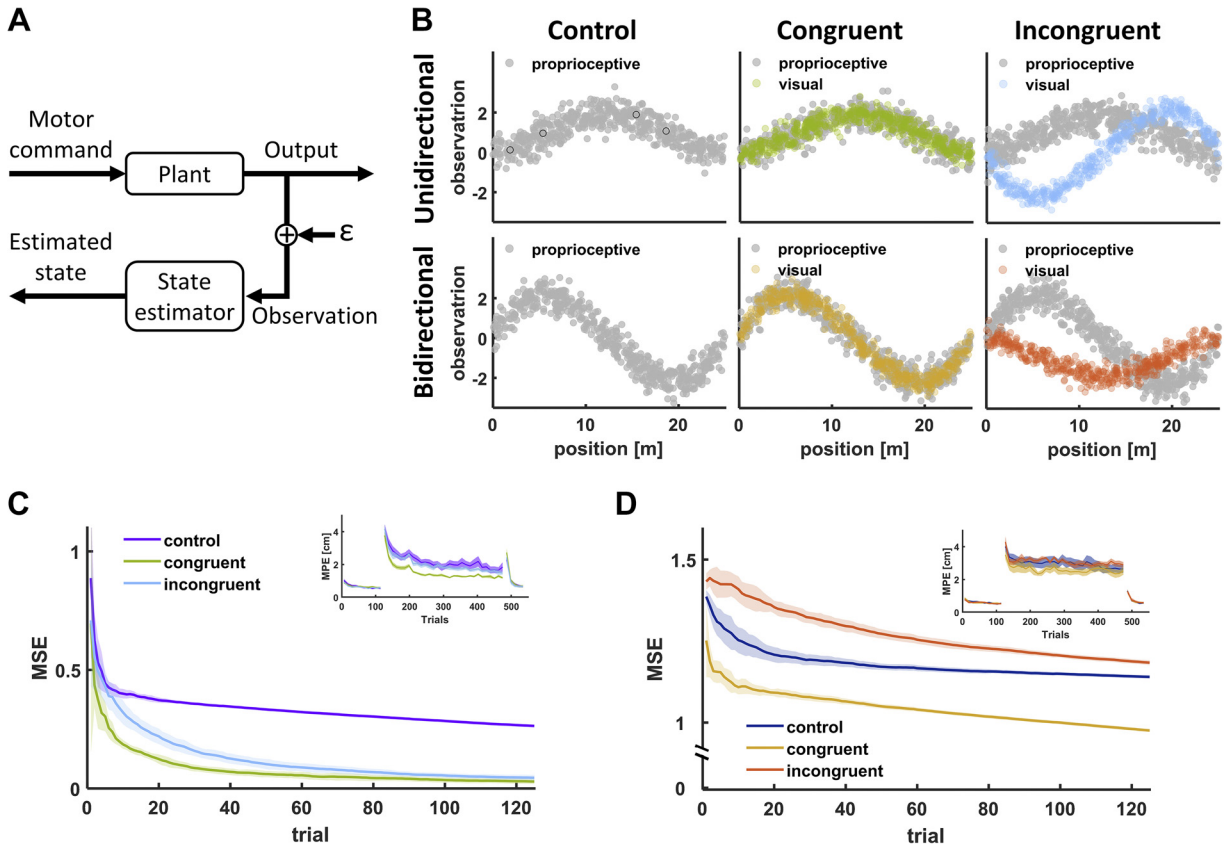

Figure 6. State estimation-based adaptation. *A*: block diagram of state estimation. The motor command sent from the brain changes the state of the arm (plant), which is sensed by multiple sensory modalities such as proprioception or visual. The role of the state estimator is to estimate the state using integration between information sources and reduce the effect of noise (ε), which distort the sensory signals. *B*: example for simulated sensory information regarding the scaling factor k for each experimental condition across all trials. In each trial, we simulated that the system acquires four randomly chosen data points, for example, the four data points marked using black circles in the *top left* panel. Top row of panels represents examples for proprioceptive (gray dots) and visual (green dots for congruent and light blue dots for incongruent conditions) information when the force field is unidirectional. *Bottom* panels represent examples for proprioceptive (gray dots) and visual (yellow dots for congruent and red dots for incongruent conditions) information when the force field is bidirectional. *C*: difference between estimated scaling factor, $\hat{k}$, and actual value k measured using mean squared error (MSE) between the two signals for adaptation to the unidirectional force field. For the congruent condition (green line), there is a faster convergence between the true and estimated scaling factor values compared with the incongruent (light blue) and control (purple), which predicts that in this condition, participants could estimate faster and more accurate the nature of the force field. For the control condition, the visual nature of the force field is absent, which lowers the learning rate. For the incongruent condition, we simulated higher uncertainty in the scaling factor prediction, which upregulated the learning rate compared with the control condition. To compare the simulated learning trend but not the absolute values to the experimental results, Fig. 2*C* was added as an *inset*. *D*: same as *C* but for adaptation to the bidirectional force field. Here, we simulated lower uncertainty in the scaling factor prediction, which downregulated the learning rate in the incongruent condition (red curve) compared with the congruent (yellow curve) and control (blue curve). To compare the simulated learning trend to the experimental results, Fig. 2*A* was added as an *inset*.

responses of additional visual cues regarding the forces—constant, congruent with the dynamics (cues matched with the type of force field), or incongruent with the dynamics. We observed higher adaptation levels for groups that adapted to the unidirectional force field compared with groups that adapted to the bidirectional force field. For both force field types, the groups in which the visual cues were congruent with the type of force field exhibited faster learning and also a higher adaptation level at the end of learning. When the visual feedback was conflicting or not informative, the adaptation rate and final adaptation level were reduced. The comparison between the conflicting and not informative conditions did not yield a consistent effect as evident by the contradicting results we found using different analysis methods. These results demonstrated that the characteristics of motor learning can change with additional visual information regarding the nature of the environment.

There is contradicting evidence regarding the role of visual feedback in motor planning or adaptation. Congenitally blind individuals are able to adapt rapidly to novel dynamics in the complete absence of visual feedback (2). Similarly, studies have shown that people learn both stable and unstable dynamics equally well both with and without visual feedback (3, 4, 43). However, previous studies have also shown that visual information can alter motor plans and can have a great impact on motor behavior. For example, visual feedback provides useful information for dynamical control in particular to select different internal models of objects (44). Visual feedback has also been shown to be responsible for learning the direction of the movement and path planning during adaptation (4). Indeed participants experiencing a visuomotor rotation paradigm are able to successfully perform the task without proprioceptive feedback, leading to the conclusion that the visual signal enables remapping of the planned movement direction (45).

The influence of visual feedback on motor control is not limited to humans; even jumping spiders move their head toward moving objects when their lateral eye captures the motion to use their principal eyes to define the event. The retinae of the spider not only provide information about the existence of external stimuli but also its precise orientation, which is translated into a sequence of instructions to orient the spider appropriately (46). In humans, there is some evidence that movements are planned in a manner that suggests the prioritization of visual feedback for certain tasks. For example, Flanagan and Rao (47) have shown that the human brain will modify the movement path to provide a straight path in visual space. Similarly, participants will perform strongly curved movements to obtain sufficient visual feedback about the movement (48). However, visual feedback does not take into account motion of the endpoint. It has been shown that our planned trajectory is based on the visual geometric information of the entire system, not just the endpoint, by using a novel mapping between finger movements and object movement (49). In terms of adapting simultaneously to two opposing force fields, certain types of visual feedback can be used as a contextual cue to separate the learning of these dynamics (18, 19, 24, 50, 51). The fact that only specific types of contextual information allow the learning of two opposing force fields suggests that only specific signals trigger a switch between or access specific motor memories in a given task.

Compared with most previous studies of learning novel dynamics, in which the visual information provided feedback about motion errors due to the force field or cued that a different force field would be applied, in this study, we examined how additional visual information regarding the nature of the force field can affect adaptation. In this case, participants could potentially ignore the added information, especially for the incongruent visual feedback condition and have similar adaptation as with no additional visual feedback. Despite this, we found that the visual information affected adaptation. This might indicate that participants automatically process the visual representation of the forces regardless of the congruency with the underlying dynamics. This is in line with other results of manipulating objects while experiencing incongruent visual feedback. For example, incongruent visual information regarding the tip of an inverted pendulum decreased the ability of participants to stabilize the pendulum despite having reliable haptic information regarding the mechanical properties of the pendulum (52, 53). The inability to discard the incongruent visual information suggests involvement of unconscious learning processes in which this visual information can enhance or reduce the learning rate.

Indeed, several studies suggested that visual feedback triggers a more conscious, explicit strategy of action when adapting to external dynamics. That is the deviation of the visual representation of the hand, usually a cursor, from the desired straight line movement allowed participants to identify the force nature, such as the force direction, and aim or move differently. For example, Hwang et al. (17) showed that visual information about hand position but not proprioceptive information can make participants aware of the presence of a force field. They showed that this awareness caused an improvement in learning for both cases where visual information was reliable and when it was not. However, this study examined visual information, which was directly linked with the motion error due to forces. In a recent study, Zhou and colleagues (54) contrasted motor learning performance between two experimental groups in a reach adaptation task to assess the extent to which explicit visual feedback facilitates motor learning. Specifically, one group of participants experienced a velocity-dependent force field (i.e., received both visual and proprioceptive feedback), whereas the other group moved in force channels and was provided visual feedback concerning the lateral force they produced as well as the force required to overcome the force field (i.e., plotted the velocity-dependent force field curve). They found that decay was faster in the group that only received explicit visual feedback, although the single-trial recall was similar between the two groups. The authors concluded that motor adaptation can rely on explicit visual feedback, although adaptation, in this case, is less stable than that based on experiencing multisensory errors following physical perturbations. Although this study provided online visual feedback of the forces during the movement, the visual traces remained on the screen until after the end of the movement. This is slightly different than previous work which provided a visual picture of the forces before the start of the movement (22). Both of these are quite different to the approach of our study in which only the instantaneous visual feedback was connected to the dynamics of the environment. As we know that continuous and terminal feedback affects learning in a very different manner (55), it is possible that all of these studies produce changes in adaptation through different mechanisms.

There have been varying reports of the effectiveness of visual cues on dual adaptation. While some studies have suggested that color cues can be used to predict and compensate for switches in dynamics (20–22), more recent work has shown that color cues have limited effectiveness in such switching and updating of motor memories (18, 19). In contrast, other visual cues such as visual motion (18), visual lead-in direction (23, 24), and visual feedback location (18, 19, 25) exhibit strong effectiveness as a cue. It has been suggested that cues can be either direct or indirect in their nature (19), where direct cues contain direct information about the dynamic state of the body driving strong implicit adaptation, whereas indirect cues need to form an association with the dynamics leading primarily to an explicit adaptation on short time scales. Our current study provides online visual information regarding the time-varying state of the dynamics throughout the movement. We propose that such information should reflect a direct cue regarding the dynamics suggesting any additional effects of the congruent or incongruent nature of the cues is likely implicit in nature. However, as we only study a single direction of movement and do not directly measure the implicit and explicit contributions, we cannot confirm this suggestion.

To explain the experimental results, we proposed a computational model that predicts the pattern of adaptation based on a state estimation. In this model, the state estimator forms a representation of the external force field by integrating proprioceptive information with additional visual information that represents the pattern of external forces. The state estimator receives information from the two modalities and updates the representation of the environment as more information is

accumulated. Since the proprioceptive sensory input was always reliable, the model eventually converges to the coefficients values which set the force field regardless of the additional visual information. Our model suggests that the learning rate and the adaptation steady-state value depend on the uncertainty levels we have of the external dynamics representation. That is, when the two sources of information are in agreement, such as in the congruent condition, the state estimator is more uncertain in the current representation and thus changes more rapidly the estimation based on new observations. This is in line with other state estimation-based adaptations (32, 33) in which the learning rate was altered with changes in the noise in the sensory feedback. Here, however, since we did not alter sensory noise but provided multiple sensory inputs with different levels of congruency between them, we suggest a complementary way of controlling adaptation rate, which also supports the idea of a Kalman filter (42) as a way of implementing state estimator-based adaptation.

A second assumption of the suggested state estimation adaptation model is the difference in uncertainty levels according to the complexity of the force field. For the incongruent condition, we assumed a higher ability of the model to modify the representation of the scaling factor for the unidirectional force field compared with the bidirectional force field. This allowed different adaptation patterns in the incongruent condition between these two types of force fields. We suggest that in less complex force fields, such as the unidirectional field, participants were able to better learn the force pattern despite the incongruent additional visual information. Similar to increased generalization ability of low complexity force fields (56) or higher adaptation rate when visual cues are less variable (57), we suggest that the complexity of the unidirectional force pattern was low enough so to have different adaptation nature such as the ability to disregard or depress the effect of the additional visual information. For the congruent and control conditions, the model predicted different levels of estimation despite setting the uncertainty level to have the same value between unidirectional and bidirectional fields. This was consistent with the experimental results and suggests that in general, the bidirectional force field was more difficult to estimate and that it might require much more extensive training to achieve the same level of adaptation.

When people are exposed to a fully or partially unknown environment, any information about the characteristics of the environmental dynamics is valuable. Both visual and proprioceptive feedback can be used both to estimate the current state of the body and information about how to correct the movements to minimize the error. Here, we have shown that even additional visual signals can be used to increase adaptation to novel dynamics when such information relates to the dynamics of the environment. In this study, it is unclear whether such an effect was driven by changes in explicit or implicit learning. However, the computational model also replicated the experimental differences across conditions. This model suggested that the major difference was the use of this additional visual information to improve state estimates during adaptation. While this is only one possible explanation, out of many, for the results, it would suggest a more implicit explanation for the effect of congruent visual cues on the speed of adaptation. This matches with recent work suggesting a strong component of implicit learning in force field adaptation (19, 58). However, it may be that the additional visual information affected explicit learning since we did not see differences in the aftereffects according to the experimental condition (59). It is important to note that the additional visual cues are removed during the aftereffect trials, so we might expect to find no differences in the aftereffect measures regardless of the explicit or implicit nature of these effects. Further studies would be needed to confirm whether these visual cues are used within state estimation as we suggest with our model. One possible test of this would be to investigate the role of these online visual cues in dual adaptation paradigms (18) as we have suggested that strength of contextual cues depends on their use within state estimation (19, 23, 50, 51, 60). While we can only speculate on the mechanism that drives this increase in adaptation, it is clear that congruent visual cues increase the adaptation to novel dynamics compared with either incongruent or the absence of visual cues. Such effects might be useful for rehabilitation or training, especially if they can contribute through improved state estimation.

DATA AVAILABILITY

Source data for this study are openly available at https://doi.org/10.6084/m9.figshare.22923446.v1.

SUPPLEMENTAL DATA

Supplemental Video S1: https://doi.org/10.6084/m9.figshare.22843799.

ACKNOWLEDGMENTS

We thank Yang Wang with input on the experimental design, and Kevin S. H. Teo and Vijay Maharajan for their help with the experimental recordings.

DISCLOSURES

No conflicts of interest, financial or otherwise, are declared by the authors.

AUTHOR CONTRIBUTIONS

D.W.F. conceived and designed research; S.F. and D.W.F. performed experiments; S.F., R.L., M.D., and D.W.F. analyzed data; S.F., R.L., M.D., and D.W.F. interpreted results of experiments; R.L. and D.W.F. prepared figures; S.F., R.L., and D.W.F. drafted manuscript; S.F., R.L., M.D., and D.W.F. edited and revised manuscript; S.F., R.L., M.D., and D.W.F. approved final version of manuscript.

REFERENCES

1. **Farshchiansadegh A**, **Ranganathan R**, **Casadio M**, **Mussa-Ivaldi FA.** Adaptation to visual feedback delay in a redundant motor task. *J Neurophysiol* 113: 426–433, 2015. doi:10.1152/jn.00249.2014.
2. **DiZio P**, **Lackner JR.** Congenitally blind individuals rapidly adapt to coriolis force perturbations of their reaching movements. *J Neurophysiol* 84: 2175–2180, 2000. doi:10.1152/jn.2000.84.4.2175.
3. **Franklin DW**, **So U**, **Burdet E**, **Kawato M.** Visual feedback is not necessary for the learning of novel dynamics. *PLoS One* 2: e1336, 2007. doi:10.1371/journal.pone.0001336.
4. **Scheidt RA**, **Conditt MA**, **Secco EL**, **Mussa-Ivaldi FA.** Interaction of visual and proprioceptive feedback during adaptation of human

reaching movements. *J Neurophysiol* 93: 3200–3213, 2005. doi:10.1152/jn.00947.2004.
5. **McKenna E**, **Bray LCJ**, **Zhou W**, **Joiner WM.** The absence or temporal offset of visual feedback does not influence adaptation to novel movement dynamics. *J Neurophysiol* 118: 2483–2498, 2017. doi:10.1152/jn.00636.2016.
6. **Westling G**, **Johansson RS.** Factors influencing the force control during precision grip. *Exp Brain Res* 53: 277–284, 1984. doi:10.1007/BF00238156.
7. **Lukos J**, **Ansuini C**, **Santello M.** Choice of contact points during multidigit grasping: effect of predictability of object center of mass location. *J Neurosci* 27: 3894–3903, 2007. doi:10.1523/JNEUROSCI.4693-06.2007.
8. **Leib R**, **Karniel A**, **Nisky I.** The effect of force feedback delay on stiffness perception and grip force modulation during tool-mediated interaction with elastic force fields. *J Neurophysiol* 113: 3076–3089, 2015. doi:10.1152/jn.00229.2014.
9. **Wolpert DM**, **Ghahramani Z**, **Jordan MI.** An internal model for sensorimotor integration. *Science* 269: 1880–1882, 1995. doi:10.1126/science.7569931.
10. **Melendez-Calderon A**, **Masia L**, **Gassert R**, **Sandini G**, **Burdet E.** Force field adaptation can be learned using vision in the absence of proprioceptive error. *IEEE Trans Neural Syst Rehabil Eng* 19: 298–306, 2011. doi:10.1109/TNSRE.2011.2125990.
11. **Sarlegna FR**, **Malfait N**, **Bringoux L**, **Bourdin C**, **Vercher J-L.** Force-field adaptation without proprioception: can vision be used to model limb dynamics? *Neuropsychologia* 48: 60–67, 2010. doi:10.1016/j.neuropsychologia.2009.08.011.
12. **Lefumat HZ**, **Miall RC**, **Cole JD**, **Bringoux L**, **Bourdin C**, **Vercher J-L**, **Sarlegna FR.** Generalization of force-field adaptation in proprioceptively-deafferented subjects. *Neurosci Lett* 616: 160–165, 2016. doi:10.1016/j.neulet.2016.01.040.
13. **Yousif N**, **Cole J**, **Rothwell J**, **Diedrichsen J.** Proprioception in motor learning: lessons from a deafferented subject. *Exp Brain Res* 233: 2449–2459, 2015. doi:10.1007/s00221-015-4315-8.
14. **Tsay JS**, **Chandy AM**, **Chua R**, **Miall RC**, **Cole J**, **Farnè A**, **Ivry RB**, **Sarlegna FR.** Implicit motor adaptation and perceived hand position without proprioception: a kinesthetic error may be derived from efferent signals (Preprint). *bioRxiv*, 2023. doi:10.1101/2023.01.19.524726.
15. **Hermsdörfer J**, **Elias Z**, **Cole JD**, **Quaney BM**, **Nowak DA.** Preserved and impaired aspects of feed-forward grip force control after chronic somatosensory deafferentation. *Neurorehabil Neural Repair* 22: 374–384, 2008. doi:10.1177/1545968307311103.
16. **Miall RC**, **Rosenthal O**, **Ørstavik K**, **Cole JD**, **Sarlegna FR.** Loss of haptic feedback impairs control of hand posture: a study in chronically deafferented individuals when grasping and lifting objects. *Exp Brain Res* 237: 2167–2184, 2019. doi:10.1007/s00221-019-05583-2.
17. **Hwang EJ**, **Smith MA**, **Shadmehr R.** Dissociable effects of the implicit and explicit memory systems on learning control of reaching. *Exp Brain Res* 173: 425–437, 2006. doi:10.1007/s00221-006-0391-0.
18. **Howard IS**, **Wolpert DM**, **Franklin DW.** The effect of contextual cues on the encoding of motor memories. *J Neurophysiol* 109: 2632–2644, 2013. doi:10.1152/jn.00773.2012.
19. **Forano M**, **Schween R**, **Taylor JA**, **Hegele M**, **Franklin DW.** Direct and indirect cues can enable dual adaptation, but through different learning processes. *J Neurophysiol* 126: 1490–1506, 2021. doi:10.1152/jn.00166.2021.
20. **Krouchev NI**, **Kalaska JF.** Context-dependent anticipation of different task dynamics: rapid recall of appropriate motor skills using visual cues. *J Neurophysiol* 89: 1165–1175, 2003. doi:10.1152/jn.00779.2002.
21. **Addou T**, **Krouchev N**, **Kalaska JF.** Colored context cues can facilitate the ability to learn and to switch between multiple dynamical force fields. *J Neurophysiol* 106: 163–183, 2011. doi:10.1152/jn.00869.2010.
22. **Osu R**, **Hirai S**, **Yoshioka T**, **Kawato M.** Random presentation enables subjects to adapt to two opposing forces on the hand. *Nat Neurosci* 7: 111–112, 2004 [Erratum in *Nat Neurosci* 7: 314, 2004]. doi:10.1038/nn1184.
23. **Howard IS**, **Franklin DW.** Neural tuning functions underlie both generalization and interference. *PLoS One* 10: e0131268, 2015. doi:10.1371/journal.pone.0131268.
24. **Howard IS**, **Wolpert DM**, **Franklin DW.** The value of the follow-through derives from motor learning depending on future actions. *Curr Biol* 25: 397–401, 2015. doi:10.1016/j.cub.2014.12.037.
25. **Hirashima M**, **Nozaki D.** Distinct motor plans form and retrieve distinct motor memories for physically identical movements. *Curr Biol* 22: 432–436, 2012. doi:10.1016/j.cub.2012.01.042.
26. **Körding KP**, **Wolpert DM.** Bayesian integration in sensorimotor learning. *Nature* 427: 244–247, 2004. doi:10.1038/nature02169.
27. **Bays PM**, **Wolpert DM.** Computational principles of sensorimotor control that minimize uncertainty and variability. *J Physiol* 578: 387–396, 2007. doi:10.1113/jphysiol.2006.120121.
28. **Hayashi T**, **Kato Y**, **Nozaki D.** Divisively normalized integration of multisensory error information develops motor memories specific to vision and proprioception. *J Neurosci* 40: 1560–1570, 2020. doi:10.1523/JNEUROSCI.1745-19.2019.
29. **van Beers RJ**, **Wolpert DM**, **Haggard P.** When feeling is more important than seeing in sensorimotor adaptation. *Curr Biol* 12: 834–837, 2002. doi:10.1016/s0960-9822(02)00836-9.
30. **Dimitriou M.** Enhanced muscle afferent signals during motor learning in humans. *Curr Biol* 26: 1062–1068, 2016. doi:10.1016/j.cub.2016.02.030.
31. **Dimitriou M.** Task-dependent modulation of spinal and transcortical stretch reflexes linked to motor learning rate. *Behav Neurosci* 132: 194–209, 2018. doi:10.1037/bne0000241.
32. **Wei K**, **Koerding K.** Uncertainty of feedback and state estimation determines the speed of motor adaptation. *Front Comput Neurosci* 4: 11, 2010. doi:10.3389/fncom.2010.00011.
33. **Burge J**, **Ernst MO**, **Banks MS.** The statistical determinants of adaptation rate in human reaching. *J Vis* 8: 20.1–20.19, 2008. doi:10.1167/8.4.20.
34. **Bernardi NF**, **Darainy M**, **Bricolo E**, **Ostry DJ.** Observing motor learning produces somatosensory change. *J Neurophysiol* 110: 1804–1810, 2013. doi:10.1152/jn.01061.2012.
35. **Oldfield RC.** The assessment and analysis of handedness: the Edinburgh inventory. *Neuropsychologia* 9: 97–113, 1971. doi:10.1016/0028-3932(71)90067-4.
36. **Howard IS**, **Ingram JN**, **Wolpert DM.** A modular planar robotic manipulandum with end-point torque control. *J Neurosci Methods* 181: 199–211, 2009. doi:10.1016/j.jneumeth.2009.05.005.
37. **Scheidt RA**, **Reinkensmeyer DJ**, **Conditt MA**, **Rymer WZ**, **Mussa-Ivaldi FA.** Persistence of motor adaptation during constrained, multi-joint, arm movements. *J Neurophysiol* 84: 853–862, 2000. doi:10.1152/jn.2000.84.2.853.
38. **Milner TE**, **Franklin DW.** Impedance control and internal model use during the initial stage of adaptation to novel dynamics in humans. *J Physiol* 567: 651–664, 2005. doi:10.1113/jphysiol.2005.090449.
39. **Franklin DW**, **Osu R**, **Burdet E**, **Kawato M**, **Milner TE.** Adaptation to stable and unstable dynamics achieved by combined impedance control and inverse dynamics model. *J Neurophysiol* 90: 3270–3282, 2003. doi:10.1152/jn.01112.2002.
40. **Smith MA**, **Ghazizadeh A**, **Shadmehr R.** Interacting adaptive processes with different timescales underlie short-term motor learning. *PLoS Biol* 4: e179, 2006. doi:10.1371/journal.pbio.0040179.
41. **Franklin DW**, **Batchelor AV**, **Wolpert DM.** The sensorimotor system can sculpt behaviorally relevant representations for motor learning. *eNeuro* 3: ENEURO.0070-16.2016, 2016. doi:10.1523/ENEURO.0070-16.2016.
42. **Kalman RE.** A new approach to linear filtering and prediction problems. *J Basic Eng* 82: 35–45, 1960. doi:10.1115/1.3662552.
43. **Tong C**, **Wolpert DM**, **Flanagan JR.** Kinematics and dynamics are not represented independently in motor working memory: evidence from an interference study. *J Neurosci* 22: 1108–1113, 2002. doi:10.1523/JNEUROSCI.22-03-01108.2002.
44. **Gordon AM**, **Westling G**, **Cole KJ**, **Johansson RS.** Memory representations underlying motor commands used during manipulation of common and novel objects. *J Neurophysiol* 69: 1789–1796, 1993. doi:10.1152/jn.1993.69.6.1789.
45. **Bernier P-M**, **Chua R**, **Bard C**, **Franks IM.** Updating of an internal model without proprioception: a deafferentation study. *Neuroreport* 17: 1421–1425, 2006. doi:10.1097/01.wnr.0000233096.13032.34.
46. **Land MF.** Orientation by jumping spiders in the absence of visual feedback. *J Exp Biol* 54: 119–139, 1971. doi:10.1242/jeb.54.1.119.
47. **Flanagan JR**, **Rao AK.** Trajectory adaptation to a nonlinear visuomotor transformation: evidence of motion planning in visually perceived space. *J Neurophysiol* 74: 2174–2178, 1995. doi:10.1152/jn.1995.74.5.2174.
48. **Yeo S-H**, **Franklin DW**, **Wolpert DM.** When optimal feedback control is not enough: feedforward strategies are required for optimal control with active sensing. *PLoS Comput Biol* 12: e1005190, 2016

[Erratum in *PLoS Comput Biol* 13: e1005370, 2017]. doi:10.1371/journal.pcbi.1005190.

49. **Danziger Z**, **Mussa-Ivaldi FA.** The influence of visual motion on motor learning. *J Neurosci* 32: 9859–9869, 2012. doi:10.1523/JNEUROSCI.5528-11.2012.
50. **Howard IS**, **Ingram JN**, **Franklin DW**, **Wolpert DM.** Gone in 0.6 seconds: the encoding of motor memories depends on recent sensorimotor states. *J Neurosci* 32: 12756–12768, 2012. doi:10.1523/JNEUROSCI.5909-11.2012.
51. **Howard IS**, **Franklin S**, **Franklin DW.** Asymmetry in kinematic generalization between visual and passive lead-in movements are consistent with a forward model in the sensorimotor system. *PLoS One* 15: e0228083, 2020. doi:10.1371/journal.pone.0228083.
52. **Franklin S**, **Česonis J**, **Franklin DW.** Influence of visual feedback on the sensorimotor control of an inverted pendulum. *Annu Int Conf IEEE Eng Med Biol Soc* 2018: 5170–5173, 2018. doi:10.1109/EMBC.2018.8513461.
53. **Česonis J**, **Leib R**, **Franklin S**, **Franklin DW.** Controller gains of an inverted pendulum are influenced by the visual feedback position. *Annu Int Conf IEEE Eng Med Biol Soc* 2019: 5068–5071, 2019. doi:10.1109/EMBC.2019.8857886.
54. **Zhou W**, **Kruse EA**, **Brower R**, **North R**, **Joiner WM.** Motion state-dependent motor learning based on explicit visual feedback is quickly recalled, but is less stable than adaptation to physical perturbations. *J Neurophysiol* 128: 854–871, 2022. doi:10.1152/jn.00520.2021.
55. **Heuer H**, **Hegele M.** Adaptation to visuomotor rotations in younger and older adults. *Psychol Aging* 23: 190–202, 2008. doi:10.1037/0882-7974.23.1.190.
56. **Thoroughman KA**, **Taylor JA.** Rapid reshaping of human motor generalization. *J Neurosci* 25: 8948–8953, 2005. doi:10.1523/JNEUROSCI.1771-05.2005.
57. **Howard IS**, **Ford C**, **Cangelosi A**, **Franklin DW.** Active lead-in variability affects motor memory formation and slows motor learning. *Sci Rep* 7: 7806, 2017. doi:10.1038/s41598-017-05697-z.
58. **Schween R**, **McDougle SD**, **Hegele M**, **Taylor JA.** Assessing explicit strategies in force field adaptation. *J Neurophysiol* 123: 1552–1565, 2020. doi:10.1152/jn.00427.2019.
59. **Parvin DE**, **Dang KV**, **Stover AR**, **Ivry RB**, **Morehead JR.** Implicit adaptation is modulated by the relevance of feedback (Preprint). *bioRxiv*, 2022. doi:10.1101/2022.01.19.476924.
60. **Howard IS**, **Franklin DW.** Adaptive tuning functions arise from visual observation of past movement. *Sci Rep* 6: 28416, 2016. doi:10.1038/srep28416.